Journal Pre-proofs

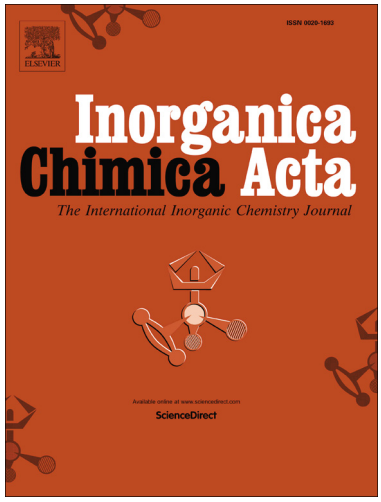

Synthesis of new triazolyl-oxazoline chiral ligands and study of their coordination to Pd(II) metal centers

Alberto Scrivanti, Roberto Sole, Marco Bortoluzzi, Valentina Beghetto, Noemi Bardella, Alessandro Dolmella

PII: S0020-1693(19)31100-4
DOI: https://doi.org/10.1016/j.ica.2019.119129
Reference: ICA 119129

To appear in: *Inorganica Chimica Acta*

Received Date: 29 July 2019
Revised Date: 3 September 2019
Accepted Date: 4 September 2019

Please cite this article as: A. Scrivanti, R. Sole, M. Bortoluzzi, V. Beghetto, N. Bardella, A. Dolmella, Synthesis of new triazolyl-oxazoline chiral ligands and study of their coordination to Pd(II) metal centers, *Inorganica Chimica Acta* (2019), doi: https://doi.org/10.1016/j.ica.2019.119129

Synthesis of new triazolyl-oxazoline chiral ligands and study of their coordination to Pd(II) metal centers

by

Alberto Scrivanti, [a,b]* Roberto Sole, [a] Marco Bortoluzzi, [a,b] Valentina Beghetto, [a] Noemi Bardella, [a] Alessandro Dolmella [c]

a) *Dipartimento di Scienze Molecolari e Nanosistemi, Università Ca' Foscari Venezia, Via Torino 155, 30172 Mestre - Italy*
b) *CIRCC, via C. Ulpiani 27, 70126 Bari - Italy*
c) *Dipartimento di Scienze del Farmaco, via Marzolo 5, 35131 Padova - Italy*

Abstract

We report an improved protocol for the synthesis of *TryOx*, a family of *N,N* chiral ligands in which a 1,2,3-triazol-4-yl moiety bears a chiral 2-oxazoline as the substituent in 4 position. *TryOx*s were successfully employed for the preparation of cationic Pd(II)-allyl of formulation $[Pd(allyl)(TryOx)]^+$ in which they behave as bidentate *N,N* chelating ligands. On the other hand, reaction of *TryOx*s with an equimolecular amount of $[PdCl_2(CH_3CN)_2]$ leads to the formation of neutral complexes which according to NMR, ESI-MS and molar mass determination (VPO) appear to be dimeric species of formulation $[PdCl(\mu Cl)(TryOx)]_2$ in which monodentate *TryOx*s link to palladium with the N atom of the oxazoline ring. X-rays diffraction studies show that upon crystallization these dimers transform into monomeric compounds of formulation $[PdCl_2(TryOx)]$ where the ligands behave as *N,N* chelating.

Treatment of the $[PdCl(\mu Cl)(TryOx)]_2$ dimers with an equivalent of *TryOx* affords mononuclear neutral dichloro species of formulation $[PdCl_2(TryOx)_2]$. X-ray diffraction studies show that the two *TryOx* units are equivalent behaving as monodentate ligands coordinated to the metal through the oxazoline *N* atom.

Keywords: oxazoline, triazole, bidentate ligands, palladium, palladium allyl complexes.

*Corresponding author, e-mail: alberto.scrivanti@unive.it

1. **Introduction**

Design and development of novel and efficient ligands is a core activity in transition-metal catalysis because organic ligands properties ultimately affect the steric and electronic characteristics of metal centers allowing to improve and tune activity, regioselectivity and (when appropriate) enantioselectivity of the metal-catalyzed reactions. Expected benefits include milder reaction conditions, improved chemo-, regio- and stereo-selectivity eventually leading to more sustainable chemical processes.

After more than 40 years, pyridine-oxazolines (*PyOx*, Scheme 1), a class of chiral *N,N*-bidentate ligands originally conceived by H. Brunner in 1980's [1,2], continue to attract chemists interest as confirmed by the recent reviews appeared in the literature [3-5].

Likewise, in the last two decades nitrogen ligands containing triazole rings drew increasing attention not only in relation with their coordination characteristics but also because their structures can be easily modified taking advantage of the modular nature of the copper catalyzed [2+3] alkyne-azide cycloaddition [6,7].

Inspired by the chemical structure of *PyOx* ligands we devised the synthesis of a novel type of chiral N,N-bidentate ligand in which a chiral oxazoline ring bears as the substituent a triazolyl moiety (Scheme 1).

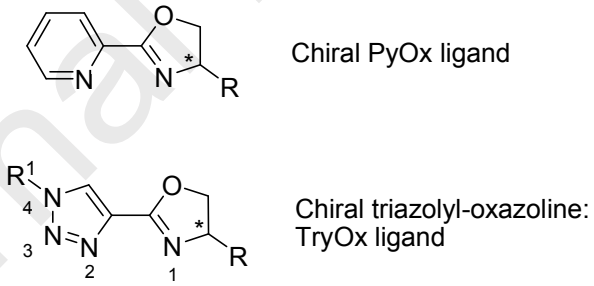

Scheme 1. Chemical structures of *PyOx* and of *TryOx* ligands

We are confident this novel class of ligands will find applications in different fields of coordination chemistry and asymmetric catalysis. In this connection, it is to remark that owing to the modular nature of triazole synthesis it will be possible to prepare libraries of these ligands allowing for a fine tuning of their characteristics.

Furthermore, it should be noted that beyond the plain structural similarity with *PyOx* ligands, *TryOx*s could display some unprecedented coordination chemistry. As a matter of fact, it is generally assumed that while the σ-donor strengths of the triazole and pyridine are not very different, pyridines are considered to be a better π acceptors than 1,2,3-triazoles. [8]. These

characteristics can be exploited in other fields; for instance in a preliminary account on the synthesis of a *TryOx* prototype [9] we have already shown that *TryOx*s can be successfully employed in combination with some lanthanides to give photoluminescent species.

We wish to report herein an improved protocol for the synthesis of chiral *TryOx* ligands and preliminary studies on their coordination to Pd(II) metal centers. Inspection of the literature reveals that achiral *TryOx* ligands (i.e. species as depicted in Scheme 1 in which R = H) have been previously synthesized by Cook [10] and by Maas [11]. In particular, it is worth to mention that Maas showed by X-ray diffraction analysis that the achiral *TryOx* having R^1 = benzyl and R = H behaves towards Cu(II) as a monodentate ligand, coordination occurring through the *N* atom of the oxazoline.

2. Experimental

2.1 Materials and instrumentation

Commercial solvents (Aldrich) were purified as described in the literature [12].

(*S*)-(+)-2-Amino-1-butanol, (*S*)-(+)-2-amino-4-methyl-1-pentanol [L-leucinol, (*S*)-(+)-leucinol], and (*S*)-(+)-2-amino-3,3-dimethylbutyric acid (L-*tert*-leucine) were purchased from Aldrich. Benzylazide [13] and *t*-butylazide [14] were prepared according to procedures reported in the literature (caution: aliphatic azides and HN_3 are explosive and toxic). 1-Benzyl-1*H*-[1,2,3]triazole-4-carboxylic acid was prepared according to the procedure described by Gautier [15]. (*S*)-(+)-2-Amino-3,3-dimethylbutanol (L-*tert*-leucinol) was synthesized by reduction of (*S*)-(+)-2-amino-3,3-dimethylbutyric acid according to a literature procedure [16]. 4-(4,6-dimethoxy-1,3,5-triazin-2-yl)-4-methylmorpholinium chloride (DMTMM) was prepared as described by Kunishima [17]. $[Pd(\eta^3\text{-}C_3H_5)Cl]_2$ was prepared according to the method described by Hartley [18]. All syntheses were carried out under inert atmosphere (nitrogen) using standard Schlenk techniques. ^1H and ^{13}C $\{^1H\}$ NMR spectra were recorded on a Bruker AVANCE 300 spectrometer operating at 300.21 and 75.44 MHz, respectively. The chemical shift values of the spectra are reported in δ units with reference to the residual solvent signal. The proton assignments were performed by standard chemical shift correlations as well as by ^1H 2D COSY experiments.

ESI-MS analyses were performed using a Finnigan LCQ-Duo ion-trap instrument, operating in positive ion mode (sheath gas N_2, source voltage 4.0 KV, capillary voltage 21 V, capillary temperature 200 °C). Sample solutions were prepared by dissolving Pd complexes (about 1 mg) in methanol (1 mL) and then further diluting with methanol (1:30). All mass spectra were recorded on freshly prepared solutions.

Elemental analyses (C, H, N) were carried out at the University of Padua using a Fison EA1108 microanalyzer.

IR spectra were collected in the range 4000 – 400 cm^{-1} using a Perkin-Elmer Spectrum One spectrophotometer.

Melting points were determined using a Büchi B-535 apparatus.

Optical rotatory power values (α) were determined using a Jasco P-2000 polarimeter (Na lamp at 25 °C).

Molar masses in solution were measured by Vapor Phase Osmometry (VPO) employing chloroform solutions (37 °C) on a Knaeur Dampfdruck Osmometer.

2.2 Ligands synthesis

(1-t-Butyl-1H-[1,2,3]triazol-4-yl) metanoic acid (**1b**)

In a mixture of *t*-BuOH (15 mL) and water (15 mL) were dissolved 1.50 g (15.00 mmol) of *t*-BuN_3 and 1.40 g (1.5 ml, 16.6 mmol) of methyl propiolate. Then, under nitrogen, were added in the order a solution of sodium ascorbate (0.29 g, 1.50 mmol) in water (2 mL) and finally a solution of $CuSO_4 \cdot 5H_2O$ in water (0.19 g, 0.75 mmol in 2 mL of H_2O). The mixture was kept under stirring and then after 24 hours it was taken to dryness. The brown solid residue was extracted with dichloromethane, filtered and taken to small volume. The resulting oil was chromatographed on silica gel (eluent: dicholoromethane/diethyl ether = 95/5) to give the methyl ester of **1b** as a white solid.

^{1}H NMR ($CDCl_3$, 298 K) δ: 8.16 (s, 1H), 3.94 (s, 3H), 1.70 (s, 9H).

The recovered ester was dissolved in MeOH (30 mL) and treated with 10 mL of an 10% aqueous NaOH solution. The mixture was stirred for 3 h, then the methanol was distilled off at reduced pressure. The aqueous phase was neutralized at pH = 7 by addition of 5% aq. HCl, and extracted with dichloromethane (3 × 30 mL). The reunited organic phases were dried upon anhydrous $MgSO_4$, filtered and taken to dryness in high vacuum to give **1b** as a white solid (1.86 g, 73% yield).

^{1}H NMR (acetone-d_6, 298 K) δ: 8.53 (s, 1H), 3.77 (b s, 1H, COOH), 1.73 (s, 9H).

^{13}C NMR ($CDCl_3$, 298 K) δ: 164.1, 138.7, 125.7, 60.8, 30.0.

(*S*)-1-*Benzyl-N-(1-hydroxy-butan-2-yl)-1H-1,2,3-triazol-4-carboxyamide* (**2a**)

In a round bottomed flask, 0.48 mL (5.00 mmol) of (*S*)-(-)-2-amino-1-butanol and 1.03 g of **1a** (5.00 mmol) were dissolved in 50 mL of acetonitrile. Then 3.00 g (5.40 mmol) of DMTMM were added to the mixture, which was kept under stirring overnight. After removing the solvent under reduced pressure, the resulting off-white solid residue was treated with 10 wt% of aq. NaOH (10 mL). The suspension thus obtained was filtered, the recovered solid was washed with H_2O and dried under vacuum to give 0.92 g of **3a** as a white powder (70% yield).

^{1}H NMR ($CDCl_3$, 298 K) δ: 7.95 (s, 1H), 7.41-7.26 (m, 5H) 7.24 (br s, 1H), 5.54 (s, 2H), 4.12-3.90 (m, 1H), 3.81-3.59 (m, 2H), 2.70 (br s, 1H, OH), 1.76-1.52 (m, 2H), 0.99 (t, 3H, *J*=6.9 Hz).

(*S)-1-(t-Butyl)-N-(1-hydroxy-4-methylpentan-2-yl)-1H-[1,2,3]-triazol-4-carboxyamide* (**2b**)

According to the above procedure, DMTMM (1.23 g, 4.10 mmol) was added to a solution of (*S*)-(+)-2-amino-4-methyl-1-pentanol (0.49 g, 4.20 mmol) and **1b** (0.70 g, 4.14 mmol) in acetonitrile (40 mL). Workup as for **2a** gives the sought amide as a white solid (0.79 g, 71% yield).

^{1}H NMR ($CDCl_3$, 298 K) δ: 8.14 (s, 1H), 7.21 (br d, 1H, *J*=8.6 Hz, NH), 4.23 (m, 1H), 3.77 (dd, 1H, *J*=11.1 and 3.6 Hz), 3.64 (dd, 1H, *J*=11.1 and 6.2 Hz), 2.83 (br s, 1H, OH), 1.72 (m, 1H), 1.69 (s, 9H), 1.63-1.34 (m, 2H), 0.95 (d, 6H, *J*=6.5 Hz).

(*S*)-*1-(t-Butyl)-N-(1-hydroxy-3,3-dimethylbutan-2-yl)-1H-[1,2,3]-triazol-4-carboxyamide* (2c)

According to the above procedures, DMTMM (1.94 g, 7.00 mmol) was added to a solution of (*S*)-(+)-2-amino-3,3-dimethylbutanol (0.82 g, 7.00 mmol) and **1b** (1.20 g, 7.00 mmol) in acetonitrile (40 mL). Workup as for **2a** allows to obtain the sought amide as a white solid (1.51 g, 81% yield).

^{1}H NMR ($CDCl_3$, 298 K) δ: 8.14 (s, 1H), 7.34 (br d, 1H, *J*=8.6 Hz, NH), 4.09-4.00 (m, 1H), 4.00-3.88 (m, 1H), 3.66 (m, 1H), 2.71 (t, 1H, *J*=11.0 Hz, OH), 1.68 (s, 9H), 1.02 (s, 9H).

(*S*)-*1-Benzyl-N-(1-chloro-butan-2-yl)-1H-[1,2,3]-triazol-4-carboxyamide* (3a)

A solution of $SOCl_2$ (0.9 mL, 12.1 mmol) in dichloroethane (10 mL) was drop wise added to a suspension of **2a** (1.66 g, 6.05 mmol) in dichloroethane (100 mL) under nitrogen at room temperature. The mixture was heated under stirring at 60 °C for 4 hours to afford a clear pale yellow solution. Upon cooling at room temperature a white solid precipitates. The liquid phase was removed in high vacuum to give a off-white powder (1.70 g, 99% yield) which was characterized by ^{1}H NMR spectroscopy and used in the following step without any further purification.

^{1}H NMR ($CDCl_3$, 298 K) δ: 7.98 (s, 1H), 7.46-7.36 (m, 5H, arom.) 7.28 (br d, 1H, *J*=8.0 Hz, NH), 5.57 (s, 2H), 4.38-4.25 (m, 1H), 3.80-3.66 (m, 2H), 1.93-1.52 (m, 2H), 1.0 (t, 2H, *J*=6.8 Hz).

(*S*)-*1-(t-Butyl)-N-(1-hydroxy-4-methylpentan-2-yl)-1H-[1,2,3]-triazol-4-carboxyamide* (3b) The compound was prepared according to the above procedure (quantitative yield).

^{1}H NMR ($CDCl_3$, 298 K) δ: 8.13 (s, 1H), 7.18 (br d, 1H, *J*=8.8 Hz, NH), 4.51 (m, 1H), 3.76 (dd, 1H, *J*=11.1 and 4.4 Hz), 3.65 (dd, 1H, *J*=11.1 and 3.9 Hz), 1.70 (s, 9H), 1.80-1.45 (m, 3H), 0.96 (d, 6H, *J* =6.4 Hz).

***(S)*-1-(*t*-Butyl)-N-(1-chloro-3,3-dimethylbutan-2-yl)-1*H*-[1,2,3]-triazol-4-carboxyamide (3c)**

The compound was prepared according to the above procedures (quantitative yield).

^{1}H NMR ($CDCl_3$, 298 K) δ: 8.16 (s, 1H), 7.20 (br d, 1H, *J*=9.6 Hz, NH), 4.29 (ddd, 1H, *J*=10.5, 9.2 and 3.4 Hz), 3.88 (dd, 1H, *J*=11.5, and 3.4 Hz), 3.56 (dd, 1H, *J*=11.5 and 9.2 Hz), 1.70 (s, 9H), 1.04 (s, 9H).

***1-Benzyl-((S)-4-ethyl-4,5-dihydrooxazol-2-yl)-1H-[1,2,3]-triazole* (4a)**

Under nitrogen, finely powdered NaOMe (1.00 g) was added to a solution of **3a** (0.58 g, 2.00 mmol) in methanol (10 mL). The resulting suspension was heated under stirring at 55 °C for 6 hours, then the solution was cooled to room temperature and taken to dryness under vacuum. The solid residue was dissolved in dichloromethane (30 mL) and the suspension thus obtained was extracted with water (4 × 30 mL). The organic phase was dried over $MgSO_4$ and then filtered. The filtrate was dried under vacuum to afford 0.41 g (81% yield) of ligand **4a** as a white solid.

^{1}H NMR ($CDCl_3$, 298 K) δ: 7.89 (s, 1H), 7.40-7.25 (m, 5H), 5.55 (s, 2H). 4.49 (dd, 1H, *J*=9.3 and 8.1 Hz,), 4.16-4.26 (m, 1H), 4.02-4.07 (m, 1H), 1.51-1.58 (m, 2H), 0.98 (t, 3H, *J*=7.4 Hz).

^{13}C NMR ($CDCl_3$, 298 K) δ: 157.0, 138.0, 133.92, 128.5, 129.2, 129.4, 124.9, 72.5, 68.1, 54.7, 28.6, 10.2.

M.p.: 86 °C. Elemental analysis: $C_{14}H_{16}N_4O$ (256.30), calcd. C, 65.61; H, 6.29; N, 21.86; found: C, 65.4; H, 6.4; N, 21.8.

GC-MS: 256 $[M]^+$, 227 $[M - C_2H_5]^+$, 156, 106, 91.

$[\alpha]_D^{25}$ = - 20.0 (c = 1, CH_2Cl_2).

IR (KBr, cm^{-1}): 3070 (m), 2952 (ms), 1672 (s), 1544 (ms), 1454 (s), 1046 (s), 1004 (ms), 883 (m), 713 (s).

1- tert-Butyl-4-((S)-1- 4-isobutyl-4,5-dihydrooxazol-2-yl)-1H-1,2,3-triazole (4b)

The compound was obtained as a pale yellow oil according to the above procedure (76 % yield).

^{1}H NMR ($CDCl_3$, 298 K) δ: 8.04 (s, 1H), 4.47 (dd, 1H, *J*=9.3 and 8.1 Hz), 4.25 (m, 1H), 3.97 (t, 1H, *J*=8.1 Hz), 1.75 (m, 1H), 1.62 (m, 1H) 1.61 (s, 9H), 1.38 (m, 1H), 0.89 (t, 6H, *J*=6.5 Hz).

^{13}C NMR ($CDCl_3$, 298 K) δ: 157.1, 136.8, 122.5, 73.2, 64.9, 60.0, 45.4, 29.9 (2C), 25.4, 22.7, 22.6.

Elemental analysis: $C_{13}H_{22}N_4O$ (250.34), calcd.: C, 62.37; H, 8.86; N, 22.38; found: C, 62.2; H, 8.9; N, 22.4.

GC-MS: 250 $[M]^+$, 193 $[M - C_4H_9]^+$, 126, 124, 57.

$[\alpha]_D^{25}$ = - 41.1 (c = 1.1, CH_2Cl_2).

IR (KBr, cm^{-1}): 2959 (s), 1664 (s), 1556 (w), 1470 (w), 1372 (m), 1226 (ms), 1150 (m), 1041 (ms), 940 (w), 826 (w), 699 (w).

2-tert-butyl-4-((S)-4-tert-butyl-4,5-dihydrooxazol-2-yl) -1H-1,2,3-triazole **(4c)**

The title compound was prepared according to the above procedures (85% yield).

^{1}H NMR ($CDCl_3$, 298 K) δ: 8.09 (s, 1H), 4.35 (dd, 1H, *J*=10.1 and 8.7 Hz), 4.22 (t, 1H, *J*=8.4 Hz), 4.02 (dd, 1H, *J*=10.1 and 8.1 Hz), 1.67 (s, 9H), 0.93 (s, 9H).

^{13}C NMR ($CDCl_3$, 298 K) δ: 157.2, 137.0, 122.5, 76.3, 68.9, 60.1, 34.0, 30.1 (3C), 26.1.

M.p.: 132 °C. Elemental analysis: $C_{13}H_{22}N_4O$ (250.34), calcd.: C, 62.37; H, 8.86; N, 22.38; found: C, 62.2; H, 8.9; N, 22.4.

GC-MS: 250 $[M]^+$, 193 $[M - C_4H_9]^+$, 126, 124, 57.

$[\alpha]_D^{25}$ = - 46.9 (c = 1, CH_2Cl_2).

IR (KBr, cm^{-1}): 3111 (w), 3067 (w), 2978 (m), 2864 (w), 1670 (s), 1550 (ms), 1461 (w), 1359 (m), 1290 (w), 1233 (s), 1156 (m), 1042 (m), 1004 (m), 953 (m), 902 (w).

2.3 Synthesis of Pd(II) allyl complexes

As an example, we report the details relevant to the synthesis of **Pd1a.**

[Pd(η^3-C_3H_5)(4a)](ClO_4) **(Pd1a)**

Under inert atmosphere, a methanol solution of $AgClO_4$ (0.16 g, 0.80 mmol in 20 mL) was drop wise added to a dichloromethane solution of $[Pd(\eta^3\text{-}C_3H_5)Cl]_2$ (145 mg, 0.40 mmol in 20 mL).

The precipitated AgCl was filtered off through celite, then a CH_2Cl_2 solution of ligand **4a** (0.20 g, 0.80 mmol in 20 mL) was added to the filtrate. The resulting pale yellow solution was stirred for 1 hour under inert atmosphere, then the solvent was evaporated under reduced pressure. The obtained solid was dissolved in a few mL of CH_2Cl_2. Addition of Et_2O afforded **Pd1a** (0.32 g, 81 % yield) as a pale yellow microcrystalline solid.

^{1}H NMR ($CDCl_3$, 298 K) δ: 8.83 (s, 1H), 7.42-7.36 (m, 5H, arom.), 5.68 (s, 2H, CH_2), 5.66 (quintet, 1H, *J*=11.7 Hz, allyl central), 4.91-4.85 (t, 1H, CH_2 oxaz), 4.61-4.47 (overlapping broad m, 3H, allyl-syn and CH oxazoline), 3.38-3.16 (br m, 2H, allyl-anti), 1.82-1.64 (m, 2H), 0.93 (t, *J*=7.0 Hz, 3H).

^{13}C NMR ($CDCl_3$, 298 K) δ: 163.2 (1C), 136.4 (1C), 133.4 (1C), 129.4 (2C), 129.2 (2C), 128.4 (1C), 126.7 (1C), 116.1 (1C, H**C**-allyl), 75.9 (1C), 65.5 (1C), 62.5 (1C, H_2**C**-allyl), 60.5 (1C, H_2**C**-allyl), 55.5 (1C), 27.6 (1C), 8.5 (1C).

M.p.: 99 °C (dec.). Elemental analysis: $C_{17}H_{21}ClN_4O_5Pd$ (502.02), calcd. C, 40.57; H, 4.21; N, 11.13; found: C, 40.1; H, 3.96; N, 10.9.

ESI-MS (m/z): calcd. for $C_{17}H_{21}N_4OPd$ ($[Pd(\eta^3\text{-}C_3H_5)(\mathbf{4a})]^+$): 403.075, found: 403.070.

Λ (1×10^{-3} M in acetone): 122 (Ω^{-1} cm^2 mol^{-1}).

IR (KBr, cm^{-1}): 3080 (s), 3029 (w), 2975 (w), 2940 (w), 2870 (w), 1753 (vw), 1657 (s), 1570 (s), 1499 (w), 1467 (m), 1458 (m), 1435 (s), 1296 (w), 1258 (m), 1137 (w), 1077 (m), 940 (w), 883 (vw), 718 (s), 690 (m), 553 (w).

[Pd(η^3-C_3H_5)(4b)](PF$_6$) **(Pd1b)**

^{1}H NMR ($CDCl_3$, 298 K) δ: 8.35 (s, 1H), 5.66 (quintet, 1H, *J*= 6.5 Hz, allyl central), 4.92 (t, 1H, *J*=9.0 Hz), 4.44 (t, 1H, *J*=7.2 Hz), 4.40-4.25 (br overlapping m, 3H, allyl-syn and CH-oxaz), 3.27 (br m, 2H, allyl-anti), 1.85-1.60 (m, 2 H), 1.74 (s, 9H), 1.54-1.41 (m, 1H), 0.96 (dd, 6H, *J*=10.6 and 5.6 Hz).

^{13}C NMR ($CDCl_3$, 298 K) δ: 164.0 (1C), 136.3 (1C), 123.8 (1C), 115.7 (H**C**-allyl), 63.6 (1C), 63.3 (1C), 61.6 (br, H_2**C**-allyl), 61.00 (br, H_2**C**-allyl), 44.9, 29.7 (3C), 25.2 (1C), 23.4 (1C), 22.0 (1C).

M.p.: 98°C (dec.). Elemental analysis: $C_{16}H_{27}F_6N_4OPPd$ (542.8), calcd. C, 35.4; H, 5.01; N, 10.32; found: C, 35.2; H, 4.96; N, 10.6.

ESI-MS (m/z): calcd. for $C_{16}H_{27},N_4OPd$ ([Pd(η^3-C_3H_5)(**4b**)]$^+$): 397.122, found: 397.140.

Λ (1×10^{-3} M in acetone) = 102 $\Omega^{-1}cm^2mol^{-1}$.

IR (KBr, cm^{-1}): 2970 m, 1670 s, 1469 m, 1424 m, 1377 m, 1238 m, 1190, 1071, 841 vs, 558 vs.

[Pd(η^3-C_3H_5)(4c)](ClO$_4$) **(Pd1c)**

^{1}H NMR ($CDCl_3$, 298 K) δ: 8.48 (s, 1H), 5.73 (br m, 1H, HC-allyl), 4.87 (t, 1H, *J*=9.5 Hz), 4.79 (dd, 1H, *J*=9.2 and 4.9 Hz), 4.47 (br s, 2H, CH_2 syn), 4.20 (dd, 1H, *J*=9.7 and 4.9 Hz), 3.48 (br d, 1H, CH anti, *J*=12.0 Hz), 3.22 (br d, 1H, CH anti, *J*=9.8 Hz), 1.78 (s, 9H, t-bu), 1.02 (s, 9H, t-bu).

^{13}C NMR ($CDCl_3$, 298 K) δ: 164.5 (1C), 136.5 (1C), 123.9 (1C), 116.1 (1C, H**C**-allyl), 74.3 (1C), 73.6 (1C), 63.8 (br, 1C, H_2C-allyl), 63.7 (1C), 62.3 (br, 1C, H_2C-allyl), 34.9 (1C), 29.8 (3C), 25.9 (3C).

Mp.: 120 °C (dec.). Elemental analysis: $C_{16}H_{27}ClN_4O_5Pd$ (496.07), calcd. C, 38.64; H, 5.47; N, 11.27; found: C, 38.4; H, 5.66; N, 11.5.

ESI-MS (m/z): calcd. for $C_{17}H_{27}N_4OPd$ ([Pd(η^3-C_3H_5)(**4c**)]$^+$): 397.122; found 397.119.

Λ (1×10^{-3} M in acetone) = 137 Ω^{-1} cm^2 mol^{-1}.

IR (KBr, cm^{-1}): 2964 s, 1656 s, 1478 s,1427 s, 1241, vs, 1193, 1047 vs, 926, 623 vs.

2.4 Synthesis of [PdCl(μ-Cl)(L)]$_2$ (Pd2a-b)

As an example we report the details relevant to the synthesis of **Pd2a**.

[PdCl(μ-Cl)(4a)]$_2$ **(Pd2a)**

Ligand **4a** (0.13 g, 0.50 mmol) was added portion wise to a suspension of $[PdCl_2(CH_3CN)_2]$ (0.13 g, 0.50 mmol) in dichloromethane (20 mL). The resulting solution was stirred under inert atmosphere at room temperature for 20 hours. The orange solution was concentrated in high vacuum to give an orange solid, that was recrystallized from dichloromethane with diethyl ether. **Pd2a** was recovered as a yellow microcrystalline powder (0.17 g, 80% yield).

^{1}H NMR ($CDCl_3$, 298 K) δ: 7.84 (s, 1H, CH try), 7.48-7.37 (m, 5H, arom.), 5.65 (d, 1H, *J*=15.0 Hz, HHC), 5.62 (d, 1H, *J*=15.0 Hz, HHC), 5.10 (t, 1H, *J*=9.1 Hz), 4.62 (dd, 1H, *J*=5.1 and 8.3 Hz), 4.45-4.34 (br m, 1H), 2.17-2.00 (br m, 1H), 1.97-1.80 (m, 1H), 0.92 (t, 1H, *J*=7.2 Hz).

^{13}C NMR ($CDCl_3$, 298 K) δ: 163.8, 137.1, 131.5, 130.1, 129.8, 129.5, 125.9, 71.0, 63.7, 56.80, 27.3, 26.6, 8.6.

M.p.: 258 °C (dec.). Elemental analysis: $C_{28}H_{32}Cl_4N_8O_2Pd_2$ (867.26), calcd. C, 38.78; H, 3.72; N, 12.92; found: C, 39.07; H, 3.92; N, 13.14. MW (VPO, $CHCl_3$): 753.

ESI-MS (m/z). Calcd. for $C_{28}H_{32}Cl_3N_8O_2Pd_2^+$: 830.979 ($[M\text{-}Cl^-]^+$); found 830.987.

IR (KBr, cm^{-1}): 3080 (s), 3029 (w), 2975 (w), 2940 (w), 2870 (w), 1753 (vw), 1657 (s), 1570 (s), 1499 (w), 1467 (m), 1458 (m), 1435 (s), 1296 (w), 1258 (m), 1137 (w), 1077 (m), 940 (w), 883 (vw), 718 (s), 690 (m), 553 (w).

[PdCl(μ-Cl)(4b)]$_2$ (**Pd2b**).

Following the above procedure complex **Pd2b** was obtained as an orange microcrystalline powder in 77 % yield.

^{1}H NMR ($CDCl_3$, 298 K) δ: 8.08 (s, 1H), 5.18 (t, 1H, *J*=8.8 Hz), 4.55 (t, 1H, *J*=8.4) 4.49-4.39 (m, 1H), 2.38 (t, 2H, *J*=13.0 Hz) 1.73 (s, 9 H), 1.64-1.41 (m, 2H) 1.00-0.90 (m, 6H).

^{13}C NMR ($CDCl_3$, 298 K) δ: 163.9, 136.7, 123.2, 78.9, 63.9, 61.8, 43.1, 29.8 (3C), 25.6, 23.7, 21.4.

M.p.:198°C (dec). Elemental analysis: $C_{26}H_{44}Cl_4N_8O_2Pd_2$ (855.33), calcd. C, 36.51; H, 5.19; N, 13.10; found: C, 36.7, H, 5.4; N, 13.2. MW (VPO; $CHCl_3$) : 725.

ESI-MS (m/z): calcd. for $C_{26}H_{44}Cl_3N_8O_2Pd_2^+$: 819.073 ($[M\text{-}Cl^-]^+$); found 819.087.

IR (KBr, cm^{-1}): 2959 (ms), 2864 (m), 1657 (s), 1575 (s), 1474 (m), 1429 (m), 1378 (m), 1246 (ms), 1201 (m), 1074 (m), 934 (w), 693 (w), 560 (w).

[PdCl(μ-Cl)(4c)]$_2$ (**Pd2c**).

Following the above procedure complex **Pd2c** was obtained as an orange microcrystalline powder in 72 % yield.

^{1}H NMR ($CDCl_3$, 298 K) δ: 9.85 (s, 1H), 4.63-4.47 (2 overlapping m, 2H), 4.34 (dd, *J*=9.7 and 5.8 Hz), 1.51 (s, 9H), 1.26 (s, 9H).

^{13}C NMR ($CDCl_3$, 298 K) δ: 161.9, 134.4, 128.6, 75.6, 70.3, 60.8, 53.6, 34.7, 29.9 (3C), 26.4 (3C).

M.p.: 200 °C (dec.). Elemental analysis: $C_{26}H_{44}Cl_4N_8O_2Pd_2$ (855.33) $[M\text{-}Cl^-]^+$; calcd. C, 36.51; H, 5.19; N, 13.10; found: C, 36.3, H, 5.5; N, 13.3. MW (VPO; $CHCl_3$): 760.

ESI-MS (m/z). Calcd. for $C_{26}H_{44}Cl_3N_8O_2Pd_2^+$: 819.073 ($[M\text{-}Cl^-]^+$); found 819.088.

IR (KBr, cm^{-1}): 2972 (br s), 1651 (s), 1563 (s), 1480 (ms), 1435 (ms), 1397 (m), 1366 (ms), 1246 (s), 1188 (ms), 1080 (s), 927 (mw), 826 (w) 738 (mw) 693 (w), 560 (w).

2.5 Synthesis of $[PdCl_2(L)_2]$ (Pd3a-b)

As an example we report the details relevant to the synthesis of **Pd3a**.

$[PdCl_2(4a)_2]$ **(Pd3a)**.

Ligand **4a** (0.26 g, 1.00 mmol) was added portion wise to a suspension of $[PdCl_2(CH_3CN)_2]$ (0.13 g, 0.50 mmol) in dichloromethane (20 mL).

The resulting solution was stirred under inert atmosphere at room temperature for 6 hours. The orange solution was concentrated in high vacuum to give an orange solid, that was recrystallized from dichloromethane with diethyl ether. **Pd3a** was recovered as a yellow microcrystalline powder (0.27 mg, 79% yield).

^{1}H NMR ($CDCl_3$, 298 K) δ: 9.85 (s, 1H, CH try), 7.51-7.27 (m, 5H, arom.), 5.70 (s, 1H, HHC), 4.65 (t, 1H, *J*=9.1 Hz), 4.48 (dd, 1H, *J*=3.8 and 9.1 Hz), 4.27 (t, 1H, *J*=8.5 Hz), 2.87 (br m, 1H), 2.09 (m, 1H), 1.14 (t, 1H, *J*=7.2 Hz).

^{13}C NMR ($CDCl_3$, 298 K) δ: 163.8, 134.6, 129.1 128.9, 128.3, 128.1, 125.3, 72.3, 67.8, 54.4, 28.0, 9.6.

M.p.: 210 °C (dec.). Elemental analysis: $C_{28}H_{32}Cl_2N_8O_2Pd$ (689.93), calcd. C, 48.74; H, 4.67; N, 16.24; found: C, 48.42; H, 4.95; N, 16.44.

ESI-MS (m/z): calcd. for $C_{28}H_{32}ClN_8O_2Pd^+$: 653.137 ($[M\text{-}Cl^-]^+$); found: 653.128.

IR (KBr, cm^{-1}): 3118 (w), 3086 (w), 2959 (mw), 2930 (w), 2883 (vw), 1676 (s), 1664 (s); 1556 (m), 1462 (m), 1385 (w), 1233 (ms), 1207 (m), 1023 (mw), 956 (w), 718 (s), 689 (w), 541 (vw).

$[PdCl_2(4b)_2]$ **(Pd3b)**

Following the above procedure complex **Pd3b** was obtained as a dark yellow microcrystalline powder in 68% yield.

^{1}H NMR ($CDCl_3$, 298 K) δ: 9.51 (s, 1H, CH try), 4.68 (t, 1H, *J*=8.8 Hz), 4.64-4.51 (m, 1H), 4.24 (t, 1H, *J*=7.8 Hz), 3.08 (br m, 1H), 1.94 (br m, 1H), 1.74 (s, 9H), 1.12 (d, *J*=6.6 Hz, 3H).

^{13}C NMR ($CDCl_3$, 298 K) δ: 160.1, 134.1, 127.0, 73.4, 65.3, 60.8, 45.0, 30.1, 25.9, 23.9, 22.1.

M.p.: 221 °C (dec.). Elemental analysis: $C_{26}H_{44}Cl_2N_8O_2Pd$ (678.01), calcd. C, 46.06; H, 6.54; N, 16.53; found: C, 45.92; H, 6.87; N, 16.819.

ESI-MS (m/z): calcd. for $C_{26}H_{44}ClN_8O_2Pd^+$: 641.231 ([M-Cl^-]$^+$); found: 641.228.

IR (KBr, cm^{-1}): 3144 (m), 2959 (br s), 1676 (s), 1651 (s), 1556 (ms), 1467 (m), 1416 (s), 1372 (s), 1302 (m), 1238 (s), 1194 (ms), 1175 (ms), 959 (m), 839 (w), 737 (mw), 699 (mw), 601 (w), 528 (w).

[PdCl$_2$(4c)$_2$] **(Pd3c)**

Following the above procedure complex **Pd3c** was obtained as a dark yellow microcrystalline powder in 72% yield.

^{1}H NMR ($CDCl_3$, 298 K) δ: 9.81 (s, 1H, CH try), 4.65-4-55 (m, 2H), 4.35 (dd, *J*=10.3, 5.9 Hz, 1H), 4.24 (t, 1H, *J*=7.8 Hz), 1.52 (s, 9H), 1.30 (s, 9H).

^{13}C NMR ($CDCl_3$, 298 K) δ: 161.9, 134.3, 128.4, 75.5, 70.3, 60.7, 34.6, 29.8, 26.4.

M.p.: 240 °C (dec.). Elemental analysis: $C_{26}H_{44}Cl_2N_8O_2Pd$ (678.01), calcd. C, 46.06; H, 6.54; N, 16.53; found: C, 45.8; H, 6.85; N, 16.79.

ESI-MS (m/z): calcd. for $C_{26}H_{44}ClN_8O_2Pd^+$: 641.231 ([M-Cl^-]$^+$); found 641.241.

IR (KBr, cm^{-1}): 3137 (w), 2966 (m), 1639 (ms), 1544 (m), 1480 (w), 1372 (ms), 1277 (ms), 1265 (s), 1169 (w), 1042 (m), 959 (w).

2.6 ***X-Ray structure determination and refinement***

Crystals suitable for the X-ray experiment of **Pd3c** and **Pd2d** were obtained by slow diffusion of diethyl ether into a dichloromethane solution (**Pd3c**, orange prisms) or by slow evaporation of dichloromethane solutions (**Pd2d**, orange needles). In the case of **Pd3c**, a fragment of irregular shape was cut from a small prism. The selected specimens were fastened on the goniometer head of an Oxford Diffraction Gemini diffractometer. The instrument was equipped with a 2K × 2K EOS CCD area detector and sealed–tube Enhance (Mo) and (Cu) X–ray sources. Data collection were performed with the *ω*–scans technique at 300(1) K for **Pd3c**, and 297.4(6) K for **Pd2d**, using graphite–monochromated MoKα (**A**, λ = 0.71073) and CuKα (**B**, λ = 1.54184) radiation in a 1024 × 1024 pixel mode and 4 × 4 (**Pd3c**) or 2 × 2 (**Pd2d**) pixel binning. Intensities were corrected with respect to absorption, Lorentz and polarization effects. An empirical multi–scan absorption correction based on equivalent reflections was performed with the scaling algorithm *SCALE3 ABSPACK*. Unit cell parameters were determined by least–squares refinement of 11690 (**Pd3c)** and 858 (**Pd2d)** reflections chosen from the whole experiment. Data collection, reduction and refinalization were performed with the CrysAlis Pro software suite [CrysAlisPro, Version 1.171.38.46 (Rigaku OD, 2015).]. The structures were solved using SHELXT [19] and refined by

full–matrix least–squares methods based on F_o^2 with SHELXL [20] in the framework of the OLEX2 software [21].

The structure of **Pd3c** has been solved in the non-centrosymmetric $P\,4_12_12$ space group, by means of the heavy atom methods. The structure of **Pd2d** was instead solved by means of intrinsic phasing in the *P*-1 space group. In **Pd3c**, the asymmetric unit is given by half of the molecule. The refined value of the Flack parameter [22-24] was 0.001(14), suggesting a correct absolute structure. Both structures are affected by a little disorder. In **Pd3c**, atoms affected are C6 and C7; in **Pd2d**, atoms involved are C4 and C5. The alternate positions of these atoms and of bounded H atoms were refined with site occupation factors constrained to sum to unity. Refined sofs for alternate positions were 0.413/0.587 in **Pd3c** and 0.253/0.747 in **Pd2d**. All non-hydrogen atoms were refined anisotropically; H atoms were refined as "riding model". Other SHELX [19] restraints (RIGU) were also applied to improve the models.

The refinement of the structure of **Pd2d** was hampered by some limitations (see Supporting Information) and the final *R* value did not drop below ca. 12% (3.71% for **Pd3c**). However, the chemical identity of the crystallized product does not look in question. Since the main purpose of the structural determination was to identify the molecular structure of the complex, we considered the proposed solution acceptable and we terminated the refinement of **Pd2d**, at this stage. The crystallographic data for **Pd2d** and **Pd3c** have been deposited at the Cambridge Crystallographic Data Center as .cif files, with CCDC numbers 1943819 and 1943820, respectively. The data can be obtained free of charge *via* www.ccdc.cam.ac.uk/data_request/cif.

2.7 *Computational details*

The geometry optimizations and energy calculations were carried out using the range-separated DFT functional ωB97X [25-27] in combination with the split-valence polarized basis set of Ahlrichs and Weigend, with Dolg's and co-workers ECP for the palladium centre [28,29]. The implicit solvation model C-PCM was added considering acetonitrile as continuous medium [30,31]. The "restricted" formalism was always applied. The stationary points were characterized by vibrational analysis, from which zero-point vibrational energies and thermal corrections (T= 298.15 K) were obtained [32]. Calculations were performed with Gaussian 09 [33], running on an Intel Xeon-based x86-64 workstation. The software Multiwfn (version 3.5) was used for population analyses [34]. Cartesian coordinates of the DFT-optimized structures are collected in a separated file.

3. Results and Discussion

3.1. Ligands synthesis

The approach developed to synthesize the new triazolyl-oxazoline ligands **4a-c** is outlined in Scheme 2.

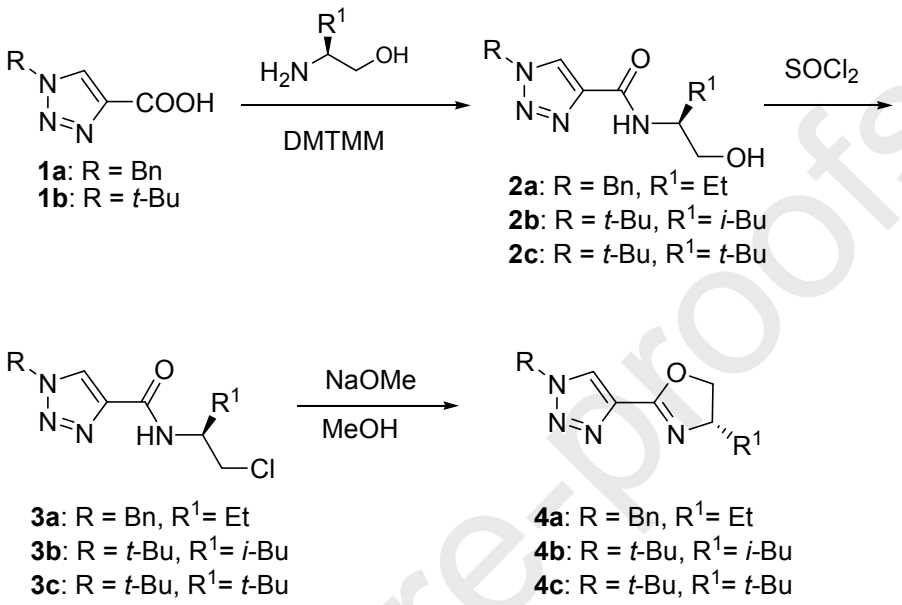

Scheme 2. Synthesis of *TryOx* ligands **4a-c**

Cu(I) catalyzed coupling of benzyl azide or *t*-butyl azide with either propiolic acid or methyl propiolate (followed by alkaline hydrolysis) is a prompt entry to prepare in high yield 1-benzyl or 1-*t*-butyl-1*H*-1,2,3-triazole-4-carboxylic acids **1a** and **1b**, respectively. Then, reaction of **1a**,**b** with chiral amino alcohols affords amides **2a-c**. Some different protocols were tested in order to improve the yield of this reaction. Best results were achieved using 4-(4,6-dimethoxy[1,3,5]triazin-2-yl)-4-methyl-morpholinium chloride (DMTMM) a stereoselective amine-carboxylic acid coupling agent [35,17]. Almost quantitative yields are achieved working at room conditions in acetonitrile, purification is simply performed by rotoevaporation of the reaction mixture followed by extraction of the residues of the coupling agent with an aqueous base.

While direct cyclization of **2a-c** to **4a-c** affords the target compounds in low yields (about 20% after chromatographic purification), the two step sequence developed by Stoltz for the synthesis of chiral *PyOx*s [5] turned out to be very efficient. Specifically, Stoltz's synthetic approach entails: i) chlorination of the amide-alcohol with $SOCl_2$, and, ii) ring closure in the presence of a base. Key features are: i) the chlorination step occurs quantitatively and does not requires any purification procedure; and, ii) the ring closure proceeds with complete retention of the

configuration at the chiral center, best yields being obtained in methanol using strong bases (e.g. 25% NaOMe). No particular problem arose in applying Stoltz's protocol to *TryOx*s synthesis; in fact, treatment of amide-alcohols **2a-c** with $SOCl_2$ gave chlorides **3a-c** quantitatively, then, treatment of **3a-c** with 10% NaOMe in methanol followed by a minimum workup allowed to obtain the sought ligands **4a-c** in 75-85% yields. Ligands **4a-c** were characterized by elemental analysis, IR, GC-MS, ^{1}H and ^{13}C NMR spectroscopies. In particular, in the ^{1}H NMR spectra the triazole proton appears as a low field singlet in the 7.89 - 8.09 range, while the protons of the oxazoline furnish three separate signals in the 4.5 – 3.8 ppm range. The relative data are reported in the Experimental section and do not deserve particular comments.

3.2. Palladium(II) complexes synthesis

3.2.1 Synthesis of Pd(II)-allyl complexes

For a first preliminary evaluation of the coordination capability of ligands **4a-c**, we choose to study the reactivity of the new ligands towards $[Pd(\eta^3\text{-}C_3H_5)Cl]_2$ in the endeavor of synthesize the corresponding Pd(II)-allyl complexes (see Scheme 3).

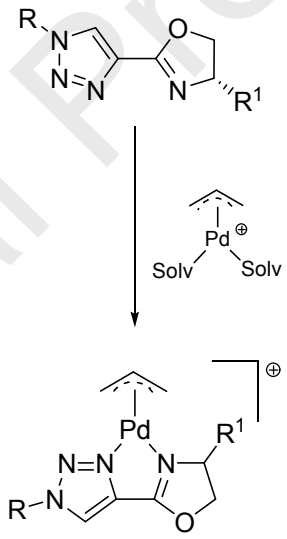

Scheme 3. Synthesis of palladium-allyl-*TryOx* complexes

As a matter of fact, nowadays palladium based catalytic processes have gained an exceptional importance in chemical synthesis and particularly in cross-coupling reactions. Among the almost infinite number of species which can be used as the catalyst or the precatalysts in palladium-catalyzed cross-coupling reactions, palladium-allyl complexes of the type $[PdX(\eta^3\text{-allyl})(L)]$ (X: anion) have a privileged position because of their stability, well established structure, and certainty of composition [36]. Moreover, the peculiar nature of the π-allyl moiety allows to use it as

coordination reporter, for instance enabling to establish through space correlations by 2D NMR techniques.

The palladium-allyl complexes **Pd1a-c** are promptly obtained by treating $[Pd(\eta^3\text{-}C_3H_5)Cl]_2$ with a silver salt (AgX: $X^- = BF_4^-$, ClO_4^-, PF_6^-) in dichloromethane; filtration of precipitated AgCl followed by addition of the ligand (Scheme 3) leads to pale yellow solutions from which the sought allyl complexes are recovered by precipitation with diethyl ether. Elemental analyses agree with the proposed formulation; in the ESI-MS spectra the most important peaks correspond to the cations $[[Pd(\eta^3\text{-}C_3H_5)(\mathbf{4a\text{-}c})]^+$, the isotope patterns being in good agreement with the calculated ones. The Λ_M of 10^{-3} M solutions of these species in acetone are in the 120-150 Ω^{-1} cm^2 mol^{-1} range confirming that these species are 1:1 electrolytes [37].

In the ^{1}H and ^{13}C NMR spectra of complexes **Pd1a-c** there are present two distinct sets of resonances which are promptly attributed to the coordinated ligand and the allyl moiety, respectively.

Comparison of the NMR chemical shifts of free and coordinated **4a-c** resonances indicates that they behave as *N,N*-chelating ligands. Coordination of the triazolyl moiety is demonstrated by a downfield shift of 0.4 – 0.8 ppm of the resonance due to the triazole ring proton, and coordination of the oxazoline ring is proved by a downfield shift of about 0.5 ppm of all the oxazoline protons.

Upon coordination to palladium, the ^{13}C NMR the signal due to the C-H of triazole is shifted downfield of about 1.3-1.8 ppm, this effect is accompanied by an upfield shift of the triazole quaternary carbon resonance which is of only about 0.5 ppm for **Pd1b**,**c** but as large as 2.0 ppm for **Pd1a**.

In the ^{1}H NMR spectra, the signals relevant to the allyl moiety are displaced to lower fields and become broad indicating dynamic behavior. In all cases, the *syn* protons give a single broad resonance, while the resonances relevant to *anti* protons appear as two broad distinct signals.

Although some different counterions (BF_4^-, ClO_4^-, PF_6^-) were employed, we didn't succeed in obtaining single crystals suitable for X-rays analysis; thus, DFT calculations were performed in order to get some deeper insights on the structural features of the allyl-complexes. The DFT-optimized structures of **Pd1a** and **Pd1c** are depicted in Figure 1, while a selection of computed bond lengths and angles is reported in the caption. The introduction of different substituents on the heterocycles causes negligible variations of the Pd-C_{allyl} bond lengths. The Pd-N2(triazole) (see Scheme 1 for atom numbering) distance is roughly the same in the two compounds, while the Pd-N(oxazoline) bond length is slightly longer in **Pd1c**, probably because of the higher steric bulk of the *t*-butyl substituent with respect to the ethyl one. As expected, no stationary points were found

trying to optimize the geometry of isomers where the ligands are coordinated by the oxazoline nitrogen and the triazole N3.

((INSERT FIGURE 1))

3. 2.2 **Synthesis of [PdCl(μCl)(L)]$_2$ (Pd2a-b)**

The picture which comes to light when *TryOxs* are allowed to react with species of the type [$PdCl_2L_2$] (L = labile ligand such as CH_3CN, BnCN or even $S(CH_3)_2$) is more intriguing; for the sake of clarity the results of our investigations are gathered in Scheme 4.

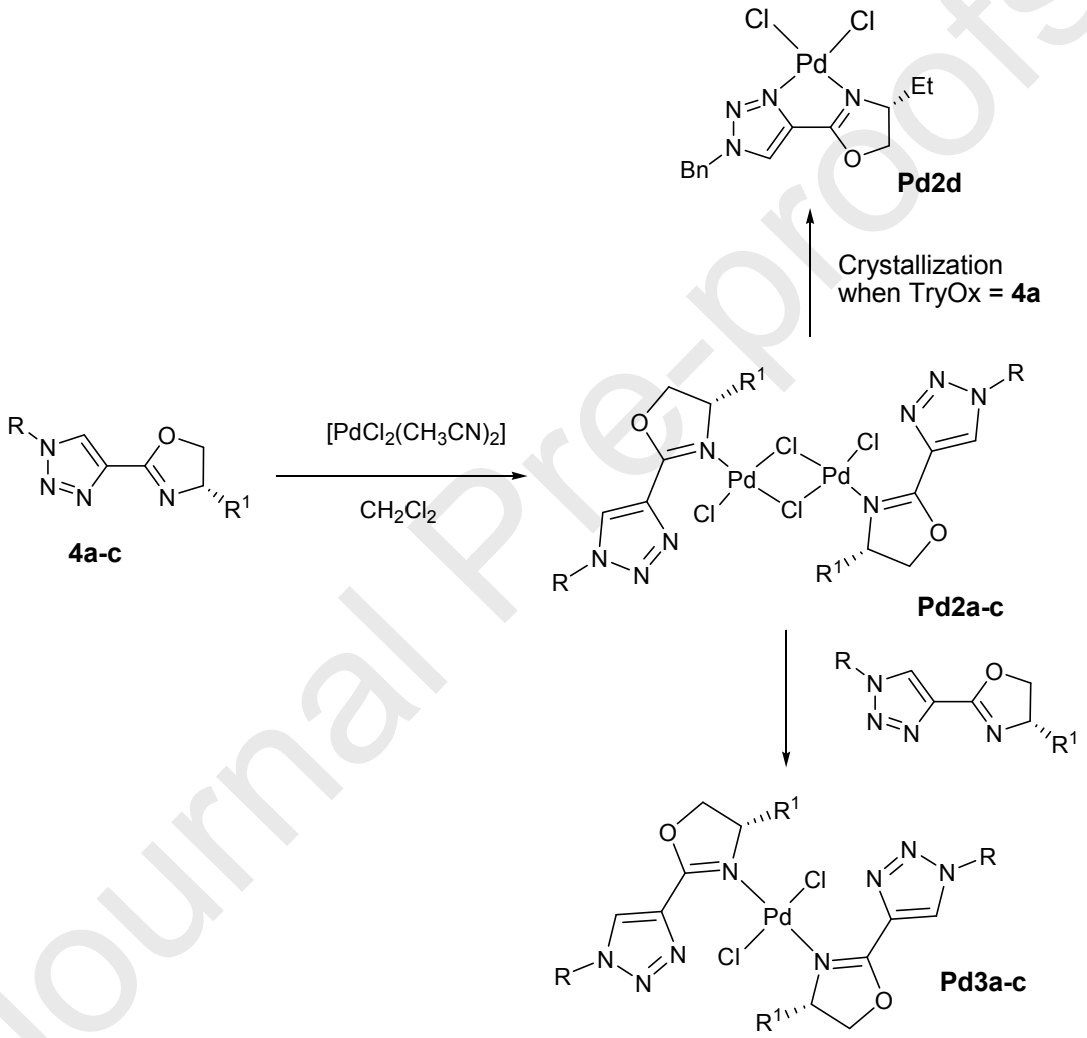

Scheme 4. Synthesis of palladium(II)-*TryOx*-chloro complexes

Treatment of [$PdCl_2(CH_3CN)_2$] with 1:1 equimolecular amounts of *TryOx*s **4a-c** in dichloromethane at room temperature affords compounds having elemental analyses in agreement with the formulation [$PdCl_2$(**4a-c**)]. The compounds are soluble in organic solvent such as dichloromethane, chloroform, tetrahydrofuran and they are non-conducting in acetone or chloroform.

In contrast with that found in the case of the cationic allyl complexes, ^{1}H NMR spectroscopy indicates that in these species *TryOx*s behaves as monodentate ligands coordinating to palladium

through the N atom of the oxazoline. Taking complex **Pd2a** as a representative example, we found that the chemical shift of the resonance due to the proton on the triazole ring is almost unaffected with respect to that of the free ligand ($\delta(CH)_{comp}$ = 7.83 *vs* $\delta(CH)_{free}$ = 7.88); on the contrary, all the resonances due to the oxazoline ring were found to give multiplets centered at 5.10, 4.60 and 4.39 δ that are significantly downfield shifted with respect the corresponding resonances of the free ligand centered at 4.44, 4.12 and 3.92 δ, respectively; the ^{1}H NMR spectra of **Pd2b** and **Pd2c** present the analogous features. The higher σ-donor ability of the oxazoline ring with respect to triazole was confirmed by the charge distribution of the ligands. The partial charge of oxazoline N in **4a** is -0.205 a.u., while that of triazole N2 is -0.152 a.u. In the case of **4c** the corresponding values are -0.198 and -0.155 a.u. The Hirshfeld population analyses supported this conclusion, the oxazoline N and triazole N2 partial charges being -0.233 and -0.162 a.u. in **4a** and -0.220 and -0.166 a.u. in **4c**.

The key indication on the nature of **Pd2a-c** in solution came from their ESI-MS. As a matter of fact, the unique clusters of signals observable in these spectra correspond to cations of formulation $[(TryOx)_2Pd_2Cl_3]^+$ suggesting that **Pd2a-c** are dimeric species (see Scheme 4) with two chlorine atoms bridging two (TryOx)PdCl units. The dimeric nature of **Pd2a-b** was definitely confirmed by determining their molecular masses in solution by Vapour Phase Osmometry.

These experimental findings are quite surprising taking into account the *N,N* chelating ability of *TryOx*s observed in the case of the above reported cationic allyl complexes; accordingly, we were intrigued to isolate crystalline samples of **Pd2a-c** suitable for X-ray diffraction analysis.

Eventually our efforts succeeded and slow evaporation of dichloromethane solutions of **Pd2a** allowed to obtain orange needles, designated as **Pd2d** in Scheme 4, that were found suitable for X-ray structural studies.

3.2.3 X–ray Crystal Structure of [$PdCl_2$(4a)] Pd2d

Summaries of crystal and structure refinement data for **Pd2d** are listed in Table I; some selected structural parameters are reported in Table II. In the latter, data for complex **Pd2d** must be regarded as preliminary.

((INSERT FIGURE 2))

Figure 2 shows the ORTEP [38] representation of **Pd2b**, with the chosen numbering scheme, with highlighted alternate positions for disordered atoms.

As noted in the Experimental section, the refinement procedure for [$PdCl_2$(**4a**)] was terminated when the final *R* index was still above 12%. In our opinion, this value is too high to

allow a discussion of the structural parameters of the molecule; hence, such discussion will not be carried over at this stage. This also apply to the disorder of the ethyl residue branching at the chiral C(3), which could hint to the possible presence of both enantiomers of the ligand. Attempts of refining the structure in the P1 space group (two molecules in cell) failed in the very early stages of the refinement, with coordinates of corresponding atoms in two independent molecules showing strong correlations, thus compelling us to perform refinement in the P-1 space group. Available data hence do not allow to confirm or reject the presence in the solid state of only one ligand enatiomer, yet are sufficient to confirm the chemical identity of the crystallized compound and the basic arrangement of the molecule, which is briefly outlined hereafter. Complex **Pd2d** is mononuclear and neutral when in the solid state. The Pd atom is bound by two chlorides and two nitrogen atoms of the chelating ligand, in a square planar environment. Upon coordination, the triazolyloxazoline ligand makes with Pd a five-membered metallacycle (N(1), C(1), C(7), N(2), Pd), with all atoms nearly coplanar. The oxazoline and triazolyl rings of the ligand also appear nearly planar. The triazolyl ring shows a slight deviation towards an envelope arrangement (with N(2) at the flap). A similar arrangement might also be expected for the partially saturated oxazoline ring, but it did not emerge at the present stage of the refinement. The mean planes encompassing the oxazoline and triazolyl rings do not perfectly coincide with the mean plane of the metallacycle, so that the molecule is slightly puckered overall (with the mean planes of oxazoline and of the triazolyl moieties bent towards each other and making a dihedral angle of about 5°). As for the benzyl residue branching at N(4), the mean plane of the phenyl ring and the mean plane of the metallacycle make with each other a dihedral angle of about 75°.

An inspection of the CCDC repository (Cambridge Structural Database, Version 5.40 of November 2018 + 3 updates) [39] for compounds having similar triazolyloxazoline ligands returned only five entries described in two papers [11,40]. Of these, one is a copper(II) compound, [11] containing two 2-(1-benzyl-1H-1,2,3-triazol-4-yl)-4,5-dihydrooxazole ligands, very similar to **Pd3c** discussed below, and three are iridium complexes of a modified benzooxazoline ligand [40]. Hence, to the best of our knowledge, this is the first report of a Pd(II) triazolyloxazoline complex.

According to the contrasting molar masses data in solution and the X-ray structure, we must conclude that while in solution **Pd2a** is a dimeric species in which the *TryOx* behaves as a monodentate ligand employing the *N* atom of the oxazoline, in the solid state, upon crystallization, it converts into **Pd2d** a mononuclear species in which the *TryOx* behaves as a *N*,*N* bidentate chelating ligand.

3..2.4 Synthesis of $[PdCl_2L_2]$ (Pd3a-b)

Taking into account the ease with which the chlorine bridge in dimeric **Pd2a** breaks**,** we were prompted to investigate the reactivity of complexes **Pd2a-c** towards the addition of a second equivalent of ligand. As a matter of fact we were intrigued to find out if a second molecule of ligand could cleave the chlorine bridges and the coordination mode adopted by the ligands in the final product.

Identical compounds of formulation $[PdCl_2(TryOx)_2]$ **(Pd3a-c**, see Scheme 4) were obtained either adding an equivalent of ligand to **Pd2a-c** or directly allowing to react $[PdCl_2(CH_3CN)_2]$ with two equivalents of ligand. Analytical data and ESI-MS are in keeping with the proposed formulation and conductivity measurements showed that complexes **Pd3a-c** are neutral compounds in chloroform or in acetone. A single set of signals is present in both the ^{1}H and ^{13}C NMR spectra of **Pd3a-c**, indicating that both *TryOx* ligands are equivalent and hence that they are coordinated to palladium in the same fashion. In the ^{1}H NMR spectra a remarkable feature is that not only the oxazoline protons, but also the triazolyl proton resonate at significantly lower fields with respect to the free ligands. Specifically, the chemical shifts of oxazoline protons are similar to these found in complexes **Pd2a-c** pointing at coordination of N atom of the oxazoline, while the triazolyl protons are found to resonate at very low fields in the 9.85 - 9.51 δ range, which is even lower than that found for the cationic complexes **Pd1a-c**. Rationalization of this puzzling spectral feature came from X-ray structural studies (see below) which demonstrate that there is a close non-bonding contact between the H atoms of triazoles and the Cl atoms of the complex.

3.2.5 X–ray Crystal Structure of Pd3c

Slow diffusion of diethyl ether into a dichloromethane solution of **Pd3c** allowed to obtain crystalline samples (orange prisms) suitable for X-ray studies. Summaries of crystal and structure refinement data for complex **Pd3c** are listed in Table I and some selected structural parameters are reported in Table II.

At the end of the refinement process the final R index (below 4%) is much better than in **[$PdCl_2$(4a)]**, leaving no unresolved peaks, especially around the chiral C(3) atom. Figure 3 shows the ORTEP representation of the compound, with the chosen numbering scheme, with highlighted alternate positions for disordered atoms.

((INSERT FIGURE 3))

Complex **Pd3c** is mononuclear and neutral. However, opposite to what found for **Pd2d**, the triazolyloxazoline ligand does not chelate Pd. Instead, two ligand units act as monodentate donors (through the N(1) atom) and the coordination environment of Pd is completed by two chloride ions. In **Pd3c**, the asymmetric unit consists of half a molecule, so the atoms belonging to the coordination plane are strictly coplanar by symmetry and the Pd coordination environment has regular square planar geometry. In the ligand, the atoms of the triazolyl ring are coplanar within 0.01 Å, while the oxazoline ring is slightly bent towards an envelope arrangement, with the C(2) atom at the flap by 0.08 Å. The position of the *tert*-butyl residue branching at the chiral C(3) atom is clearly defined, so it is ascertained that in the crystal structure of [$PdCl_2$(**4c**)$_2$] only one enantiomer of the ligand is present. The correct attribution of the absolute structure is supported, as indicated in the Experimental Section, by the value close to zero (0.001(14)) of the Flack parameter, calculated from 1576 selected quotients (Parsons' method [24]).

Opposite to what was found in **Pd2d**, the mean planes encompassing the triazolyl and oxazoline rings make with the coordination plane dihedral angles of 71.6 and 65.7°, respectively, and they also make a dihedral angle of 15.8° with each other. The reciprocal arrangement of the mean planes of the triazolyl and oxazoline moieties in reported compounds is mostly similar to that found in **Pd3c** (dihedral angles ranging from 5.4 [11] to 10.6° [40]. Among reported compounds, the entity most resembling complex **Pd3c** is the compound described in reference [11], also showing the metal bound by two monodentate ligands and two chloride ions.

With respect to bond distances in the coordination sphere, a CCDC search for mononuclear Pd(II) complexes having a PdN_2Cl_2 square planar environment (480 entries) indicates an average Pd-N, Pd-Cl distances of 2.020 Å and 2.300 Å, respectively. The values found for **Pd3c** (Pd-N bond of 2.033(2) Å, Pd-Cl lengths of 2.2913(12) and 2.3329(12) Å) look in agreement with available data. The difference between the two Pd-Cl bonds (0.042 Å) is a feature that does not appear in the pretty similar copper(II) complex [11] and points to a rather efficient intramolecular nonbonding interaction (H···Cl distance of 2.491 Å, about 0.5 Å shorter than the sum of van der Waals radii involving Cl(1) at one end and H(9) (and its symmetry equivalent at *+y,+x,1-z*) at the other. As for the triazolyloxazoline ligand, the values found in **Pd3c** of bond distances within the rings also look in reasonable agreement with the corresponding averages for reported compounds. In the triazolyl residue, the deviation between our data and mean values for corresponding bond lengths is never larger than 0.03 Å. In the oxazoline moiety there is a greater difference (largest deviation of 0.11 Å), however, most of reported complexes are in fact benzoxazoline derivatives. When looking at the closely related complex [11], the largest deviation reduces to 0.038 Å. The comparison between complex **Pd3c** and available data indicate substantial aromatic behavior in the triazolyl moiety and

no involvement in the conjugation of the C(1)-N(1) bond of the oxazoline moiety. The latter retains instead typical double bond character (1.287(3) Å, almost identical to the average of 1.289 Å for reported compounds).

Besides to the above mentioned intramolecular contact between Cl(1) and H(9), there are virtually no intermolecular contacts worth of mention. The two 'shortest' nonbonding approaches (both only 0.05 Å shorter than the sum of the pertinent van der Waals radii loosely involve the triazolyl N(2) and N(3) atoms, which respectively engage the H(12C) and the H(5B) atoms of a nearby moiety at *1.5-y, ½+x, ¼+z*. These contacts create an helical motif that propagates along with the crystallographic *b* axis.

The triazole-H---Cl interaction was also detected in the DFT-optimized structures of **Pd3a** and **Pd3c** by means of Atoms-in-Molecules (AIM) analysis. The (3,-1) bond critical points (b.c.p.) of interest are depicted in Figure 4 together with the paths connecting the (3,-1) and (3,-3) points and the interbasin surface. Selected properties at b.c.p. are reported in the Figure. In particular, the positive values of the Laplacian of electron density $\nabla^2\rho$ are in agreement with electron-unshared interactions, despite the fact that the very low negative energy density (E) values could suggest a slightly covalent nature [41].

((INSERT FIGURE 4))

Conclusions

A convenient protocol for the synthesis of triazolyl-substituted chiral oxazolines has been developed and its efficiency has been demonstrated preparing ligands having bulky and strongly electron donor substituents.

These ligands display the ability of behave both as bidentate and as monodentate, and that in this latter case that the preferred coordination site is the oxazoline *N* atom. Thus it appears that the N atom of the oxazoline is a better σ-donor than the N atoms of the triazole. Subtle effects are at play when deciding the adopted coordination fashion as found in the case of **Pd2a** → **Pd2d** transformation; further investigations are currently in progress on this subject.

Acknowledgements

Ca' Foscari University of Venice is gratefully acknowledged for financial support (Bando Progetti di Ateneo 2014, D.R. 553/2014 prot. 31352; Bando Spin 2018, D.R. 1065/2018 prot. 67416).

Conflict of interest

The authors declare that there is no conflict of interest regarding the publication of this paper.

Supplementary Information

Details about the X-ray structure refinements and Cartesian coordinates of the DFT-optimized structures are provided as Supplementary Information file.

References

[1] H. Brunner, U. Obermann, P. Wimmer, J. Organomet. Chem. 316 (1986) C1-C3.

[2] H. Brunner, U. Obermann, Chem. Ber. 122 (1989) 499–507.

[3] G. Yang, W. Zhang, Chem. Soc. Rev. 47 (2018) 1783.

[4] Z.-M. Chen, M. J. Hilton, M. S. Sigman, J. Am. Chem. Soc. 138 (2016) 11461-11464.

[5] H. Shimizu, J. C. Holder, B. M. Stoltz, Beilstein J. Org. Chem. 9 (2013) 1637–1642.

[6] L. Liang, D. Astruc, Coord. Chem. Rev. 255 (2011) 2933-2945.

[7] Q. V. C. van Hilst, N. R. Lagesse, D. Preston, Dalton Trans. 47 (2018) 997-1002.

[8] L. Suntrup, S. Klenk, J. Klein, S. Sobottka, B. Sarkar, Inorg. Chem. 56 (2017) 5771-5783.

[9] A. Scrivanti, M. Bortoluzzi, R. Sole, V. Beghetto, Chem. Pap. 72 (2018) 799-808.

[10] R. Hayashi, X. Jin, G. R. Cook, Bioorg. Med. Chem. Lett. 17 (2007) 6864-6870.

[11] S. Schröder, W. Frey, G. Maas, Z. Naturforsch. 71 (2016) 683-696.

[12] W. L. F. Armarego, D. D. Perrin, Purification of laboratory chemicals. 4th edn. Butterworth-Heinemann, Oxford, 1996

[13] P. L. Goals, N. V. Tsarevsky, K. Matyjaszewski, Macromol. Rapid Commun. 29 (2008) 1167-1171.

[14] J. C. Bottaro , P. E. Penwell, R. J. Schmitt, Synthetic Commun. 27 (1997) 1465-1467.

[15] A. Maisonial, P. Serafin, M. Traïkia, E. Debiton,V. Théry, D. J. Aitken, P. Lemoine, B. Viossat, A. Gautier, Eur. J. Inorg. Chem. (2008) 298-305.

[16] J. V. Bhaskar Kanth, M. Periasamy, J. Org. Chem. 56 (1991) 5964-5965.

[17] M. Kunishima, C. Kawachi, F. Iwasaki, K. Terao, S. Tani, Tetrahedron Letters 40 (1999) 5327-5330.

[18] F. R. Hartley, S. R. Jones, J. Organomet. Chem. 66 (1974) 465-473.

[19] G. M. Sheldrick, SHELXT - Integrated space-group and crystal-structure determination. Acta Cryst. A71 (2015).

[20] G. M. Scheldrick, Crystal structure refinement with SHELXL. Acta Cryst. C71 (2015) 3-8.

[21] OLEX2: A complete structure solution, refinement and analysis program, Version 1.2. O. V. Dolomanov, L. J. Bourhis, R. J. Gildea, J. A. K. Howard, H. Puschmann, OLEX2: a complete structure solution, refinement and analysis program. J. Appl. Cryst. 42 (2009) 339-341.

[22] G. Bernardelli, H. D. Flack, Acta Cryst. A41 (1985) 500-511.

[23] H. D. Flack, Acta Cryst. A39 (1983) 876-881.

[24] S. Parsons, H. D. Flack, T. Wagner, Acta Crystallogr., Sect. B 2013, 69, 249-259

[25] Y. Minenkov, Å. Singstad, G. Occhipinti, V. R. Jensen, Dalton. Trans. 41 (2012) 5526-5541.

[26] J.-D. Chai, M. Head-Gordon, Phys. Chem. Chem. Phys. 10 (2008) 6615-6620.

[27] I. C. Gerber, J. G. Ángyán, Hybrid functional with separated range. Chem. Phys. Lett. 45 (2005) 100-105.

[28] F. Weigend, R. Ahlrichs, Phys. Chem. Chem. Phys. 78 (2005) 3297-3305.

[29] D. Andrae, U. Häußermann, M. Dolg, H. Stoll, H. Preuß, Theor. Chim. Acta, 77 (1990) 123-141.

[30] M. Cossi, N. Rega, G. Scalmani, V. Barone, J. Comput. Chem. 24 (2003) 669-81.

[31] V. Barone, M. Cossi, J. Phys. Chem. 102 (1998) 1995–2001.

[32] C. J. Cramer, Essentials of Computational Chemistry, Wiley, Chichester, 2nd edn, 2004.

[33] M. J. Frisch, et al., Gaussian 09, Revision C.01, Gaussian Inc., Wallingford CT, USA, 2010

[34] T. Lu, F. Chen, J. Comput. Chem 33 (2012) 580-592.

[35] T. I. Al-Warhi, H. M.A. Al-Hazimi, A. El-Faham, J. Saudi Chem. Soc. 16 (2012) 97-116.

[36] D. P. Hruszkewycz, L. M. Guard, D. Balcells, N. Feldman, N. Hazari, M. Tilset, Organometallics 34 (2015) 381-394.

[37] W. J. Geary, Coord. Chem. Rev. 7 (1971) 81-122.

[38] C. K. Johnson, ORTEP, Report ORNL–5138, Oak Ridge National Laboratory, Oak Ridge, TN, 1976.

[39] F. H. Allen, Acta Cryst. B58 (2002) 380 -388.

[40] Z. Mazloomi, R. Pretorius, O. Pamies, M. Albrecht, M. Dieguez, Inorg. Chem. 56 (2017) 11282-11298.

[41] S. J. Grabowski, W. A. Sokalski, E. Dyguda, J. Leszczyński, J. Phys. Chem. B 110 (2006) 6444-6446.

Tables

Table I. Crystallographic Data for the complexes **Pd3c** and **Pd2d**.

	Pd3c	**Pd2d**
Empirical formula	$C_{26}H_{44}Cl_2N_8O_2Pd$	$C_{14}H_{16}N_4OCl_2Pd$
Formula weight	677.99	433.61
Temperature/K	300(1)	297.4(6)
Crystal system	Tetragonal	triclinic
Space group	$P\,4_1\,2_1\,2$	P-1
a / Å	9.0141(13)	7.1612(14)
b / Å	9.0141(13)	8.8314(15)
c / Å	39.596(8)	13.744(3)
α / °	90	97.653(17)
β / °	90	104.208(19)
γ / °	90	90.541(14)
Volume /Å^3	3217.3(11)	834.3(3)
Z	4	2
ρ_{calc} Mg / m^3	1.400	1.726
μ / mm^{-1}	0.779	11.972
F(000)	1408.0	432.0
Crystal size/mm^3	0.26 × 0.21 × 0.16	0.50 × 0.09 × 0.08
Reflections collected	75000	3402
Independent reflections / R_{int}	5751 / 0.0786	2093 / 0.0817
Data/restraints/parameters	5751/51/197	2093/102/208
Goodness-of-fit [a] on F^2	1.071	1.343
Final R indexes [$I > 2\sigma(I)$]	R_1 [b] = 0.0371, wR_2 [c] = 0.0673	R_1 [b] = 0.1216, wR_2 [c] = 0.3268
Largest diff. peak / hole / e Å^{-3}	0.38 / -0.73	2.63 / -1.07
Flack parameter	0.001(14)	

[a] Goodness–of–fit = $[\Sigma\,(w\,(F_o^2 - F_c^2)^2] / (N_{obsvns} - N_{params})]^{1/2}$, based on all data;

[b] $R_1 = \Sigma\,(\,|F_o| - |F_c|\,) / \Sigma\,|F_o|$;

[c] $wR_2 = [\Sigma[w\,(F_o^2 - F_c^2)^2] / \Sigma[w\,(F_o^2)^2]]^{1/2}$.

Table II: Some selected bond lengths (Å) and angles (deg) for complexes **Pd3c** and **Pd2d**

Pd3c		**Pd2d***	
Pd–Cl(1)	2.3329(12)	Pd–Cl(1)	2.288(6)
Pd–Cl(2)	2.2913(12)	Pd–Cl(2)	2.270(5)
Pd–N(1)	2.033(2)	Pd–N(1)	2.033(16)
Pd–N(1A)[a]	2.033(2)	Pd–N(2)	2.006(17)
N(1)–C(1)	1.287(3)	N(1)–C(1)	1.32(3)
N(1)–C(3)	1.502(4)		
C(1)–C(8)	1.452(5)	C(1)–C(7)	1.39(3)
C(1)–O(1)	1.346(4)		
O(1)–C(2)	1.441(5)		
C(2)–C(3)	1.516(5)		
C(8)–N(2)	1.364(4)	C(7)–N(2)	1.38(3)
N(2)–N(3)	1.310(5)	N(2)–N(3)	1.28(3)
N(3)–N(4)	1.342(4)		
N(4)–C(9)	1.343(4)		
C(9)–C(8)	1.356(5)		
Cl(2)–Pd–Cl(1)	180.00(15)	Cl(2)–Pd–Cl(1)	90.3(2)
N(1)–Pd–Cl(1)	93.38(7)	N(1)–Pd–Cl(1)	174.0(5)
N(1)–Pd–Cl(2)	86.62(7)	N(1)–Pd–N(2)	80.2(6)
N(1)–Pd–N(1A)[a]	173.24(15)	N(2)–Pd–Cl(2)	175.2(5)
N(1)–C(1)–O(1)	116.1(3)	N(1)–C(1)–C(7)	121.2(17)
C(1)–O(1)–C(2)	106.6(3)		
O(1)–C(2)–C(3)	105.6(3)		
C(3)–N(1)–C(1)	108.2(3)		
C(8)–N(2)–N(3)	107.6(3)	C(7)–N(2)–N(3)	107.5(18)
N(2)–N(3)–N(4)	108.6(3)		
N(3)–N(4)–C(9)	109.6(3)		
C(9)–C(8)–N(2)	108.6(3)		

*Data for complex **Pd2d** only preliminary; [a] at *+y, +x. 1–z*;

Captions for Figures

Figure 1. DFT-optimized structures of **Pd1a** and **Pd1c** (C-PCM/ωB97X calculations, acetonitrile as continuous medium). Color map: hydrogen, white; carbon, grey; nitrogen, blue; oxygen, red; palladium, green. Selected computed bond lengths for **Pd1a** (Å): Pd-C_{allyl}(*trans*-oxazoline) 2.110; Pd-C_{allyl}(*trans*-triazole) 2.105; Pd-C_{allyl}(central) 2.127; Pd-N(oxazoline) 2.157; Pd-N2(triazole) 2.161. Selected computed angles for **Pd1a** (°): C_{allyl}(terminal)-Pd-C_{allyl}(terminal) 69.6; N2(triazole)-Pd-N(oxazoline) 77.3; N2(triazole)-Pd-C_{allyl}(*trans*-triazole) 173.2; N(oxazoline)-Pd-C_{allyl}(trans-oxazoline) 173.0. Selected computed bond lengths for **Pd1c** (Å): Pd-C_{allyl}(*trans*-oxazoline) 2.106; Pd-C_{allyl}(*trans*-triazole) 2.108; Pd-C_{allyl}(central) 2.124; Pd-N(oxazoline) 2.182; Pd-N2(triazole) 2.157. Selected computed angles for **Pd1a** (°): C_{allyl}(terminal)-Pd-C_{allyl}(terminal) 69.4; N2(triazole)-Pd-N(oxazoline) 77.4; N2(triazole)-Pd-C_{allyl}(*trans*-triazole) 174.8; N(oxazoline)-Pd-C_{allyl}(trans-oxazoline) 176.0.

Figure 2 ORTEP drawing of **Pd2d**, showing also the numbering scheme. Thermal ellipsoids are at the 40% probability level. Hydrogen atoms are omitted for clarity; alternate positions of disordered atoms are drawn with dashed bonds.

Figure 3. ORTEP drawing of **Pd3c**, showing also the numbering scheme. Thermal ellipsoids are at the 40% probability level. Hydrogen atoms are omitted for clarity; alternate positions of disordered atoms are drawn with dashed bonds.

Figure 4. DFT-optimized structures of **Pd3a** and **Pd3c** (C-PCM/ωB97X calculations, acetonitrile as continuous medium), with H---Cl (3,-1) b.c.p. and related interbasin surface. ρ = electron density, V = potential energy density, E = electron density, $\nabla^2\rho$ = Laplacian of electron density. All quantities in a.u. Color map: hydrogen, white; carbon, dark yellow; nitrogen, blue; oxygen, red; chlorine, green; palladium, pink. Cartesian coordinates are collected in a separated file.

FIGURE 1

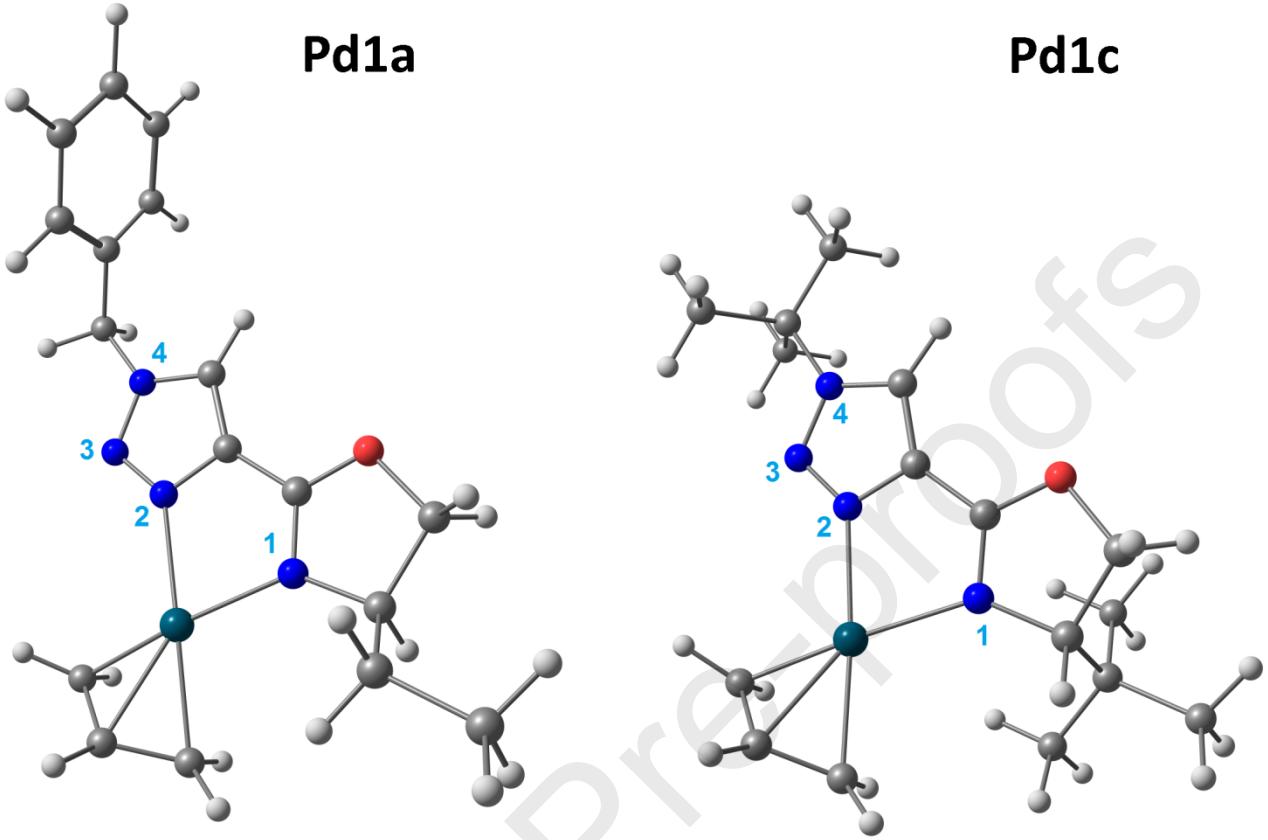

Figure 2

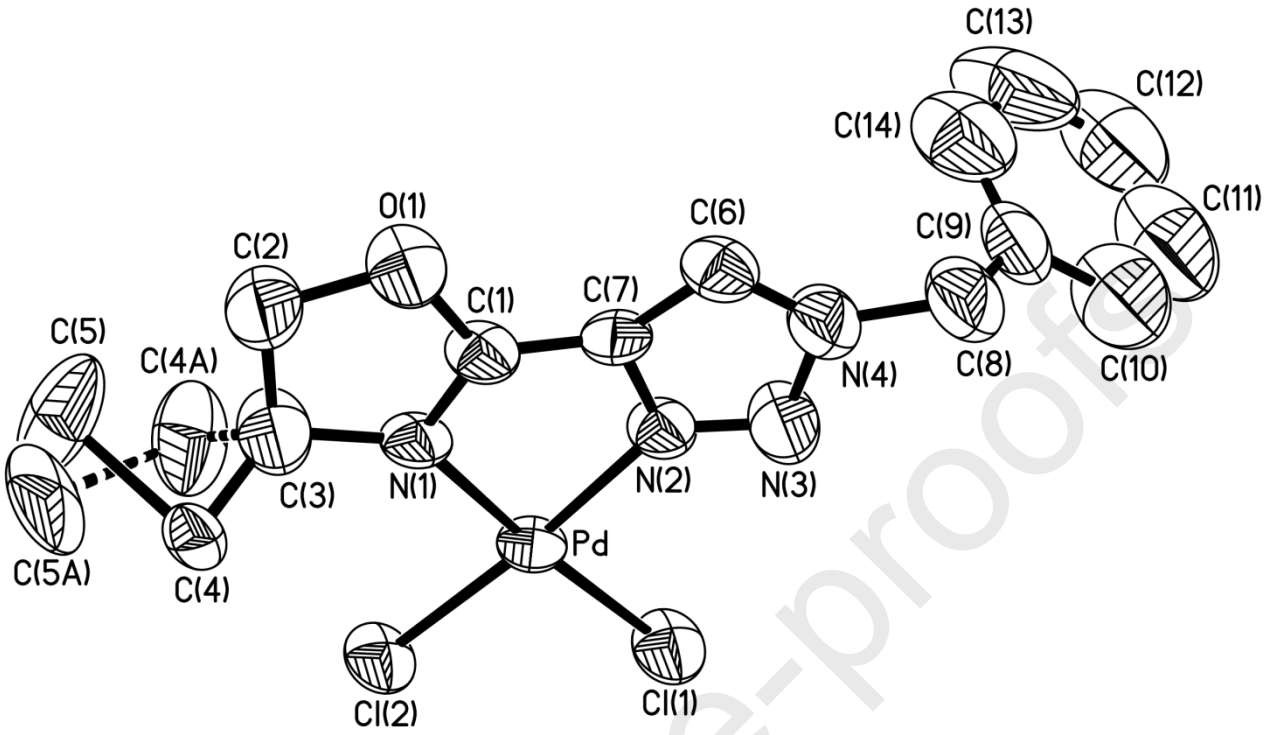

Figure 3

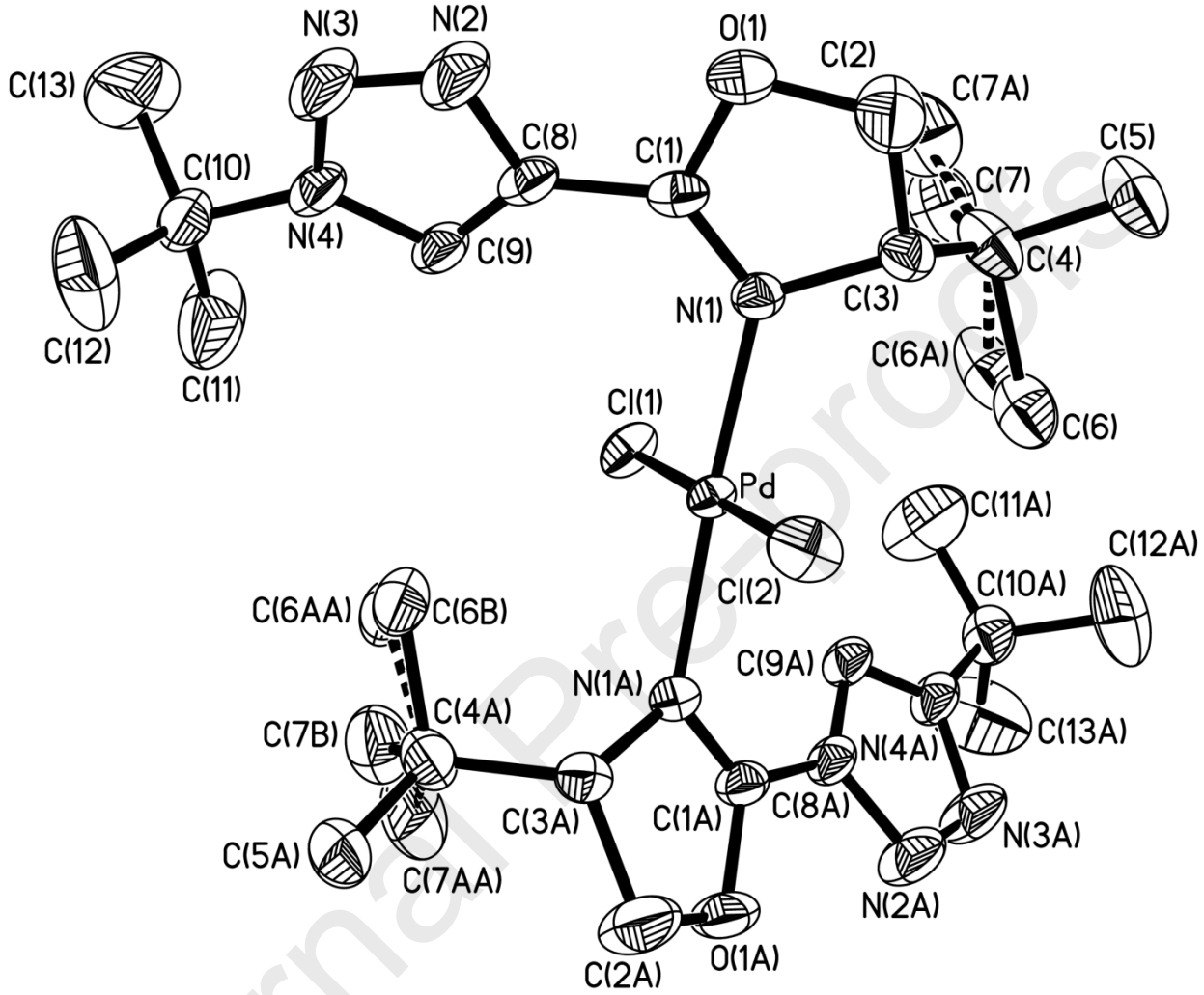

Figure 4

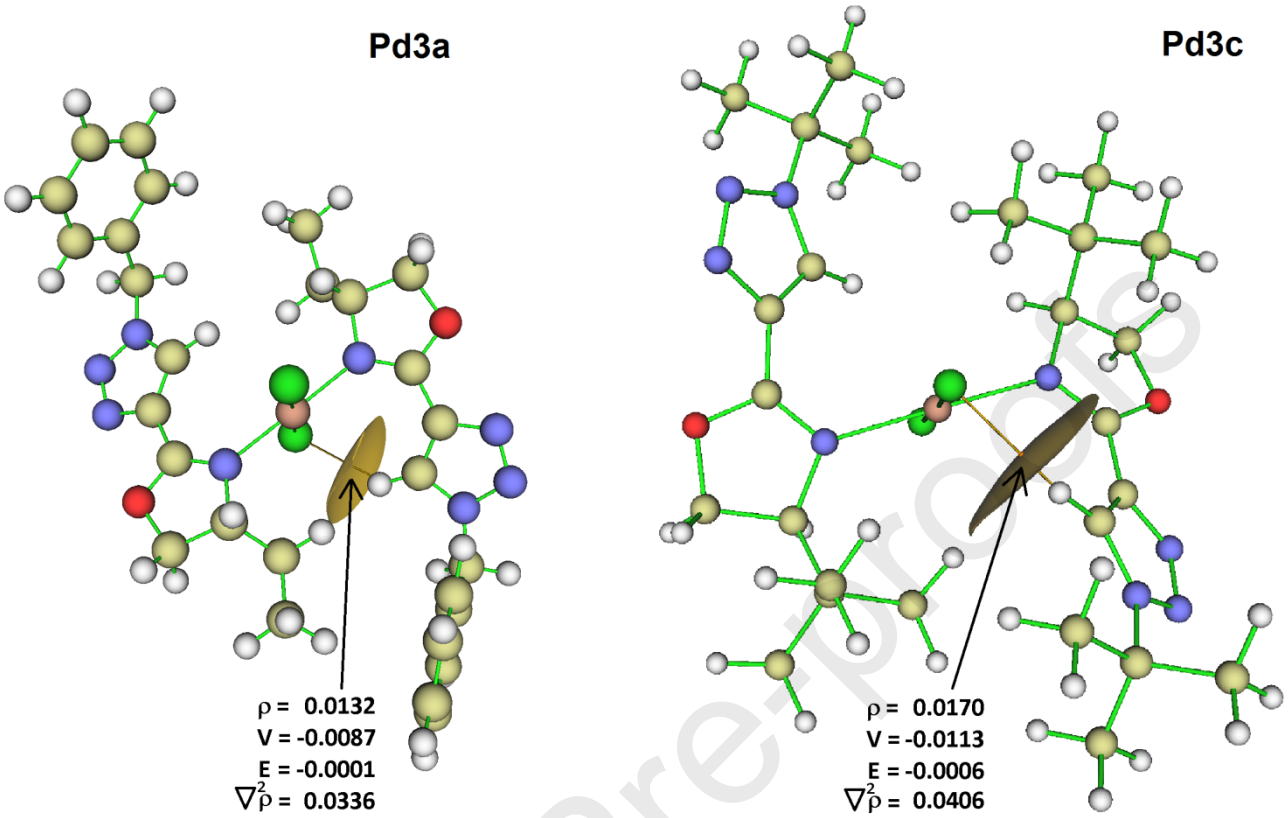

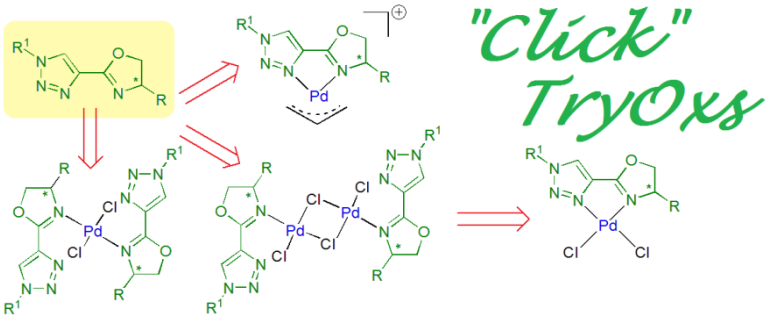

Highlights

- An improved protocol for the synthesis of triazole-oxazoline ligands is reported.
- The ligands were successfully employed for the preparation of Pd(II)-allyl complexes.
- Mono- and dimeric Pd(II) chloro-complexes were isolated.
- The oxazoline part of the ligand is the preferred ligand part for Pd(II).